磁化プラズマ中を伝播する無衝突衝撃波の生成実験：現状報告

R. Yamazaki[1], N. Ishizaka[1], S. Kakuchi[1], S. Sei[1], K. Sugiyama[1], K. Aihara[1], R. Shiina[1], Y. Sato[1], S.J. Tanaka[1], Y. Sakawa[2], T. Sano[2], M. Ota[2], S. Egashira[2], T. Izumi[2], Y. Kuramitsu[2], K. Sakai[2], T. Minami[2], T. Morita[3], S. Matsukiyo[3], M. Edamoto[3], Y. Nishioka[3], K. Tomita[4], N. Ohnishi[5], S. Tomita[5], T. Umeda[6], Y. Ohira[7], M. Hoshino[7], A. Ishii[8], and T. Takezaki[9]

[1] Aoyama Gakuin University, Japan, [2] Osaka University, [3] Kyushu University, [4] Hokkaido University, [5] Tohoku University, [6] Nagoya University, [7] University of Tokyo, [8] Max Planck Institute, [9]University of Toyama

Collisionless shocks are ubiquitous

Shocks

* are ubiquitous in various astrophysical, heliospheric, and laboratory plasmas.

* arise when two counter-streaming supersonic flows interact.

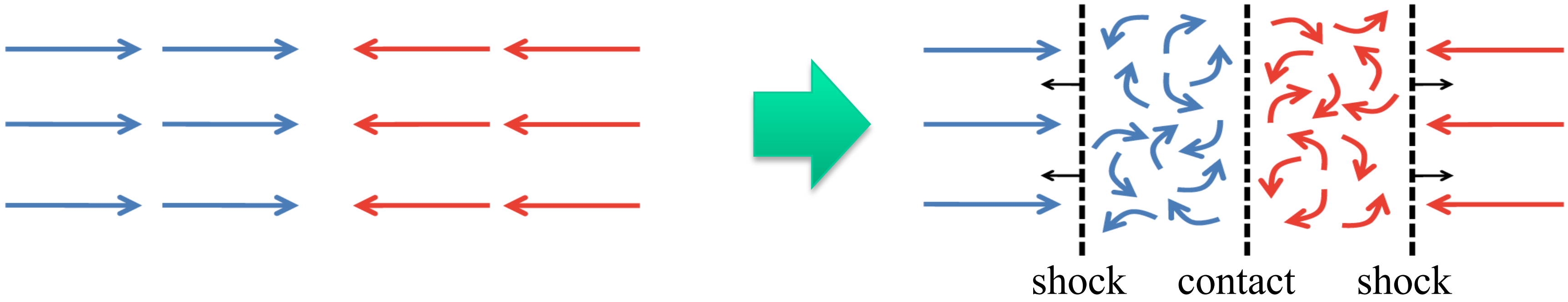

* are, in most cases, “collisionless” mainly because of low-density:
  --- Coulomb mean-free-path is much larger than the system size.
  --- Particle distribution NOT going to perfect Maxwelian.
  --- Various components arise during dissipation process.
  --- Detailed physical process of particle acceleration remains unknown.

* are, in most cases, magnetized:
  --- shocks are propagating into magnetized plasma.
  --- external magnetic field plays important roles.

Studies of collisionless shocks

Methods	Pros	Cons
Observations of astrophysical objects	▪see the whole system. ▪see evolved (t→∞). ▪less boundary effects.	▪difficult to see time evolution. ▪worse angular resolution. ▪unable to directly measure distribution functions, elemag fields.
“In-situ” observations by satellites	▪rich observables (distribution func./elemag fields). ▪short cadence	▪M~10 : uncontrolable. ▪only measurable at satellites.
Simulations	▪set initial and boundary conditions. ▪see all observables at arbitrary place and epoch.	▪huge CPU time in 3D cases ▪unrealistic parameters. ▪limited spatial and time scales
Laboratory Experiments	▪set initial and boundary conditions. ▪see all observables at arbitrary place and epoch. ▪Real parameters/physical quantities.	▪less people joining! ▪limited spatial and times scales. ▪methods unestablished.

Previous shock experiments

- Many collisional shock generation (many authors)
- Collisionless shocks in unmagnetized plasmas: w/o external B.

  --- Kuramitsu et al. (2011) with GXII: electrostatic shocks.

  --- Sakawa et al. (2019) with NIF: “Weibel” shocks.
- Collisionless shocks in magnetized plasmas: w/ external B.

  --- Paul et al. (1965) via Z-pinch: $M_A < 10$

  --- Niemann et al. (2014) with UCLA/LAPD: $M_A < 2$

  --- Schaeffer et al. (2017, 2019) with OMEGA: $M_A > \sim 10$

Our advantage over previous works:

* upstream plasma is uniform at rest, and consists of single ion.
* simple setup to have supercritical magnetized shock: $M_A > 3$.
* simultaneous measurements of density and temperature across the shock via *collective Thomson scattering*, as well as B-field.

Ion-scale structure of magnetized shock

For super-critical (M_A>3) shocks, incoming ions are reflected, making a shock "foot" at which two stream instabilities occurs (start of the shock dissipation).

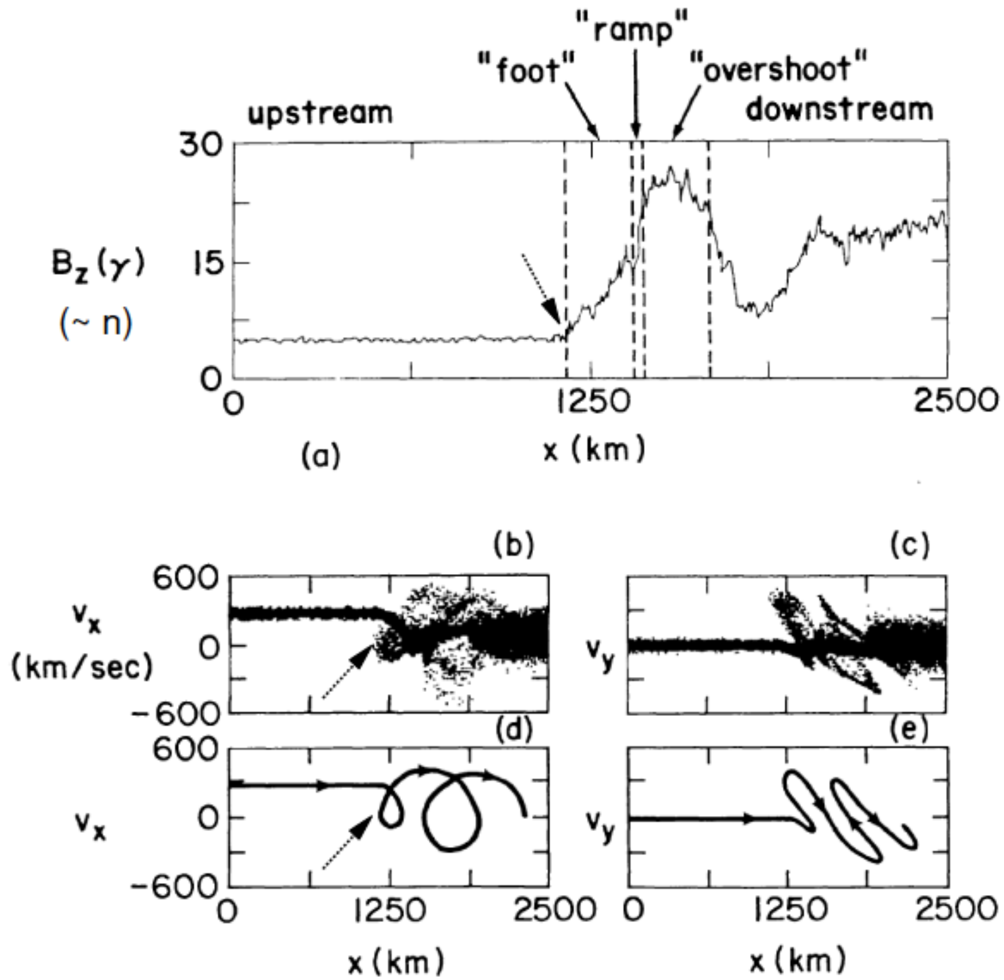

Wu et al. (1984)

1-dim PIC Simulations

Al plasmas are injected at the left boundary into the Nitrogen plasmas initially at rest.
Behavior of the driven Nitrogen plasmas depend on ambient perpendicular magnetic field.

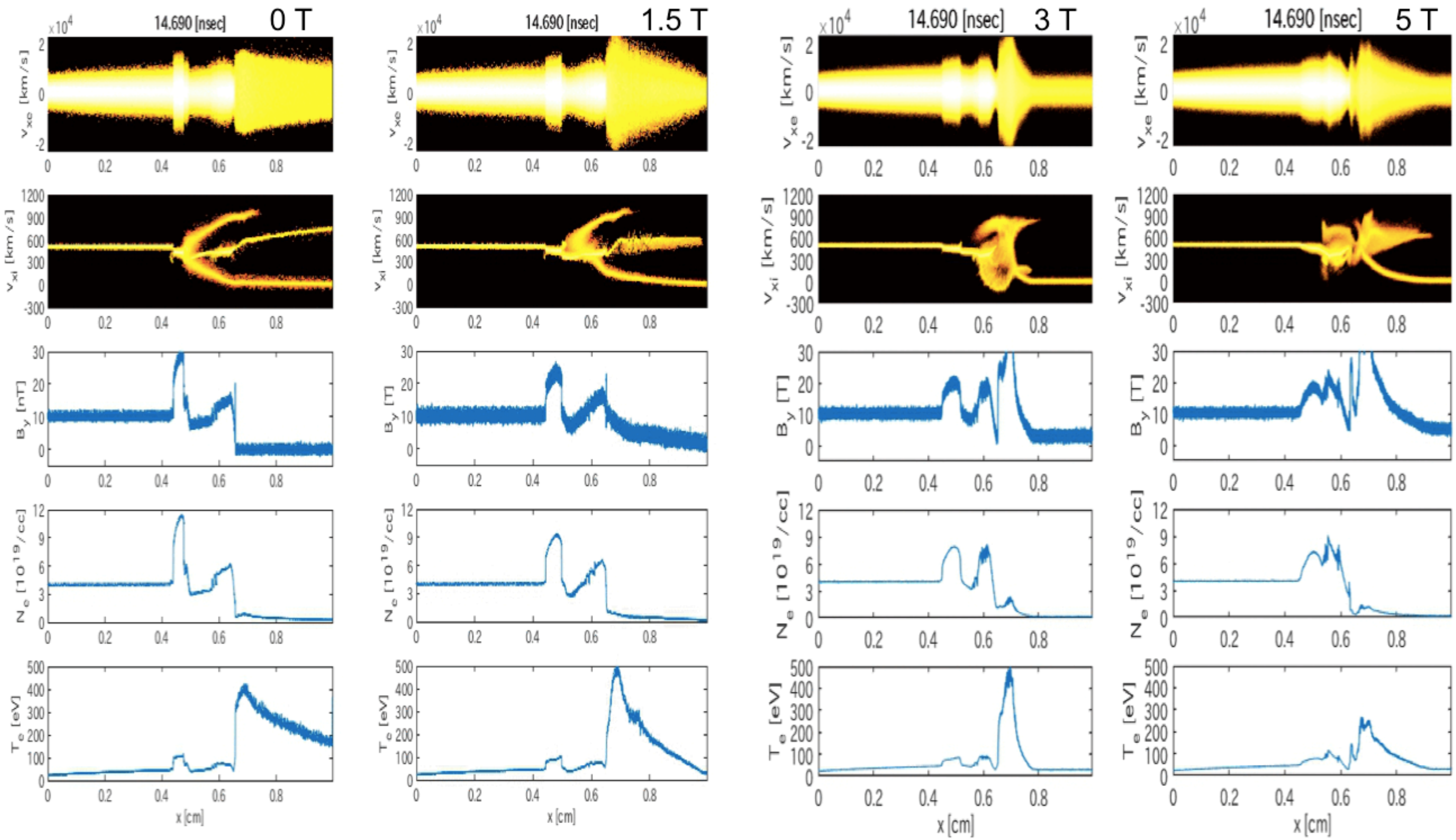

(see Umeda et al. 2019, Phys. Plasmas)

Experimental setup

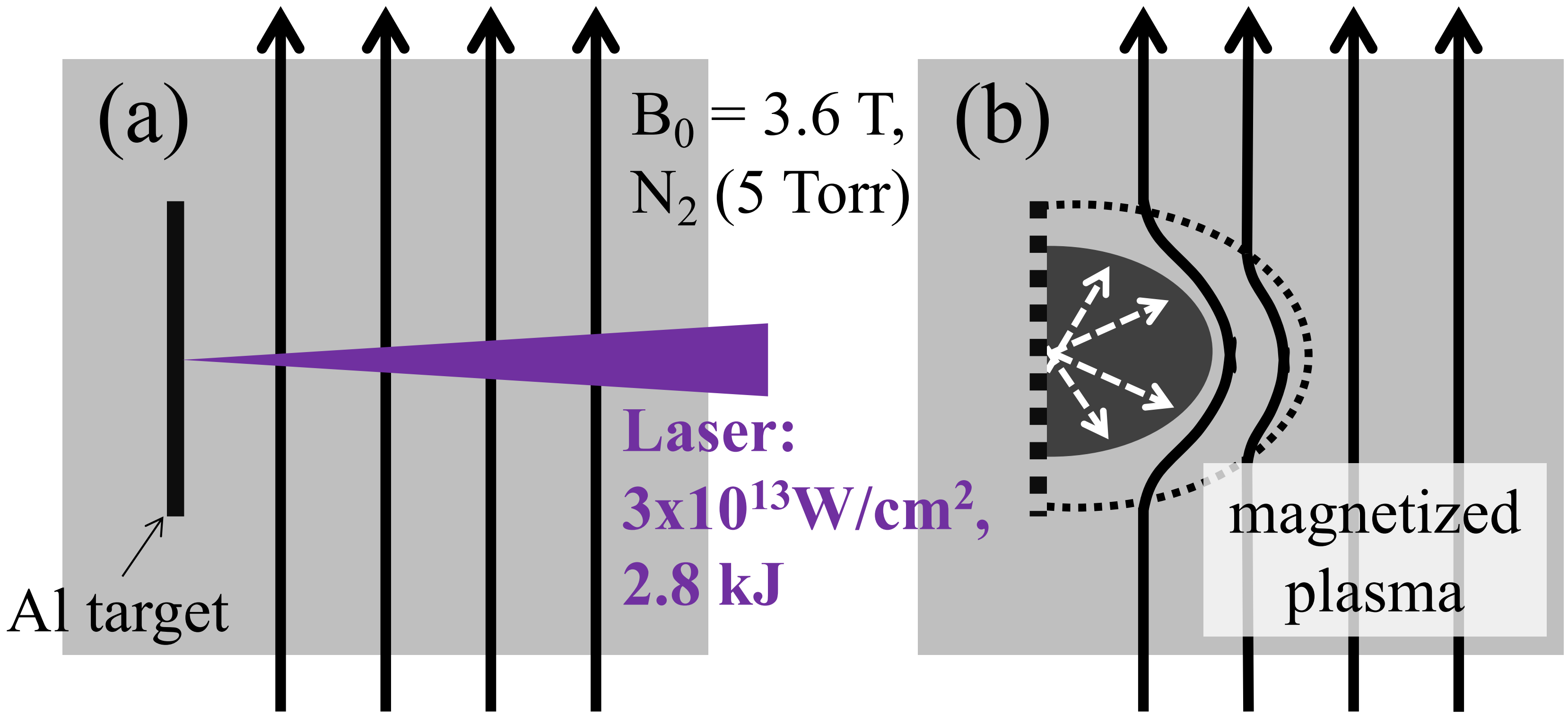

(a) Magnetic field (B_0=3.6 T: solid arrows) is applied around an Al plane target, and the target is irradiated by high-power laser.

(b) The Al target ejects plasma and ionizing photons. Ambient Nitrogen gas (5 Torr) is ionized and simultaneously magnetized. Target Al plasma pushes magnetized N plasma (white arrows) to generate a collisionless shock (dotted curve).

External magnetic field

- Edamoto et al. 2018, Rev. Sci. Instr.

  Coils: inner diam.=110 mm, 50 turns.

  (separation = 25 mm)

  Capacitors: 3 mF × 8 (V =1.4 kV)

  Imposed B-field: ~3.6 T, duration~0.1 ms.

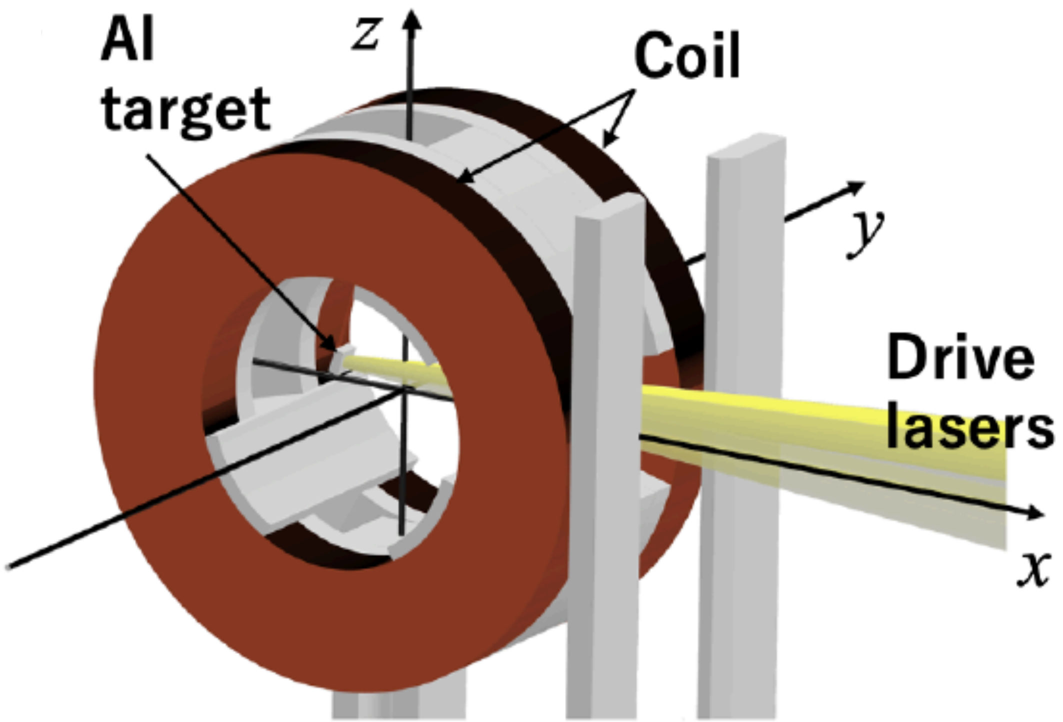

View from *y*-axis
(self-emission measurements)

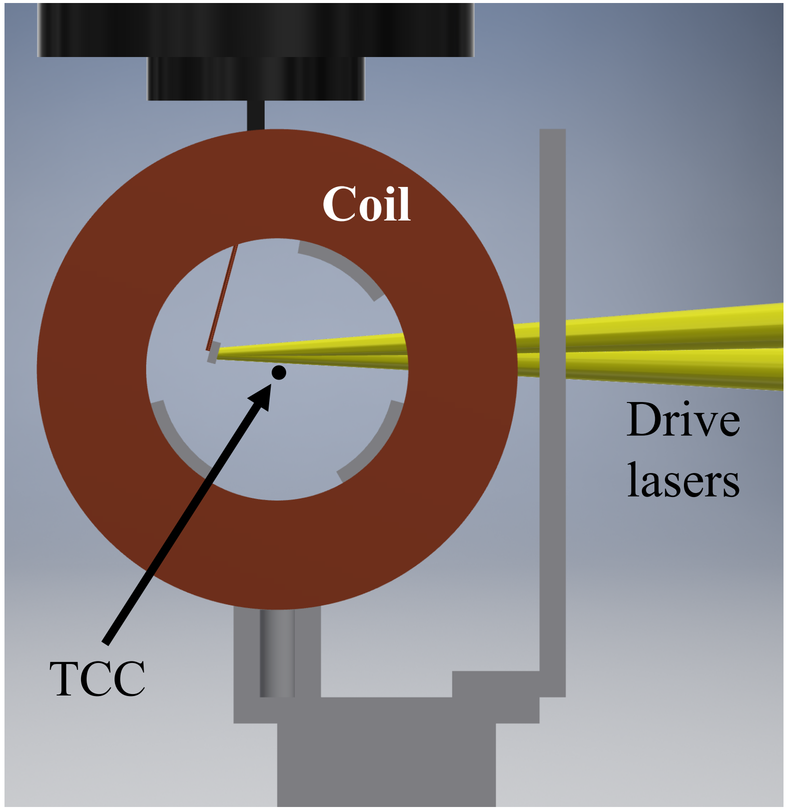

External magnetic field

- Edamoto et al. 2018, Rev. Sci. Instr.

  Coils: inner diam.=110 mm, 50 turns.
  (separation = 25 mm)
  Capacitors: 3 mF × 8 (V =1.4 kV)
  Imposed B-field: ~3.6 T, duration~0.1 ms.

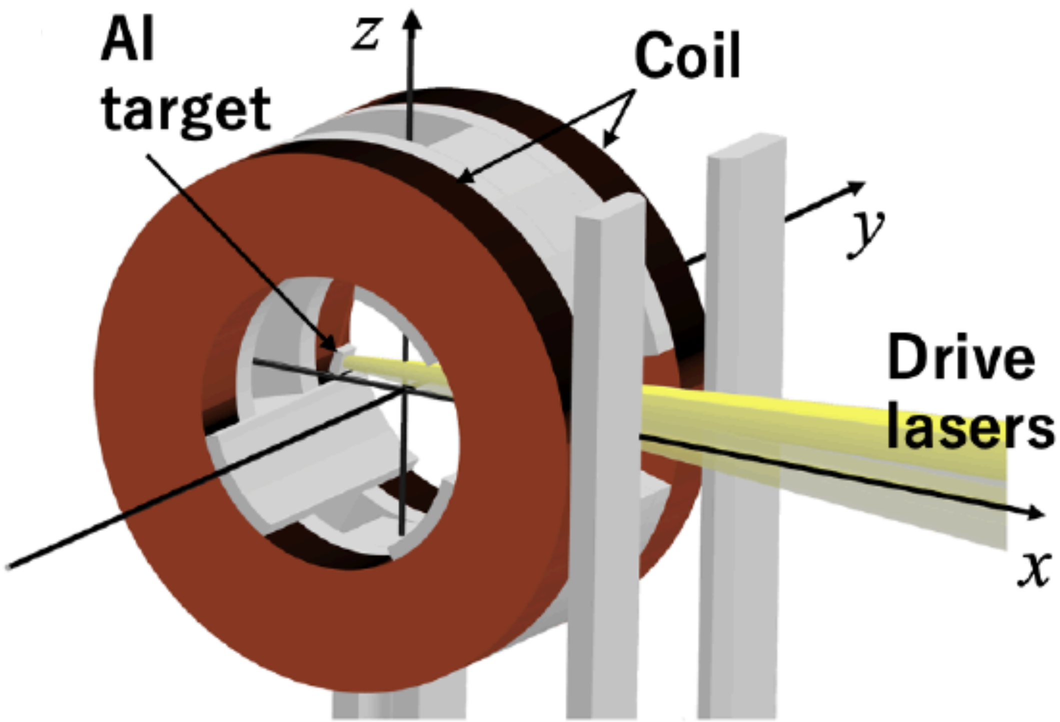

Before set into chamber

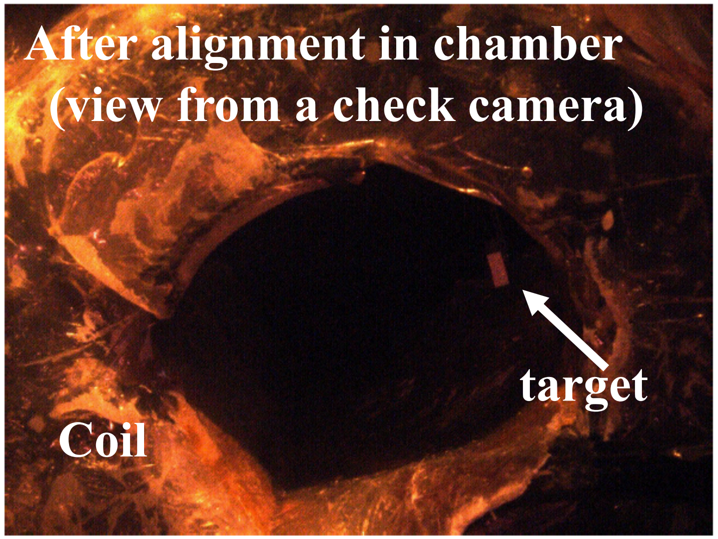

外部磁場印加の履歴

これまで印加できた外部磁場強度の変遷：

2017年度：B = 0.5 T (V = 14 kV, C = 2.7 nF x 24),　1 shot.

⇒設計(コンデンサ容量、印加電圧、コイル巻き数、大きさ等)
を抜本的に見直し。

2018年度：B = 1.6 T (V = 0.4 kV, C = 3 mF x 4),　9 shots.

2019年度：B = 3.6 T (V = 1.4 kV, C = 3 mF x 8),　1 shot.

2020年度：B = 2.9 T (V = 0.8 kV, C = 3 mF x 8),　8 shots.
B = 3.3 T (V = 1.6 kV, C = 3 mF x 8),　4 shots.

2021年度：B ~ 5 T ?? (V = 1.6 kV, C = 3 mF x 16),　??? shots.

Diagnostics

- Self emission (optical; brems & lines): from high-T regions.
- Collective Thomson scattering : T_e, T_i, n_e, Z, bulk flow velocity
- B-field measurements: B-dot w/ coil, (proton backlight)
- Particle measurements: w/ CR-39
- Others: shadowgraphy, interferometry

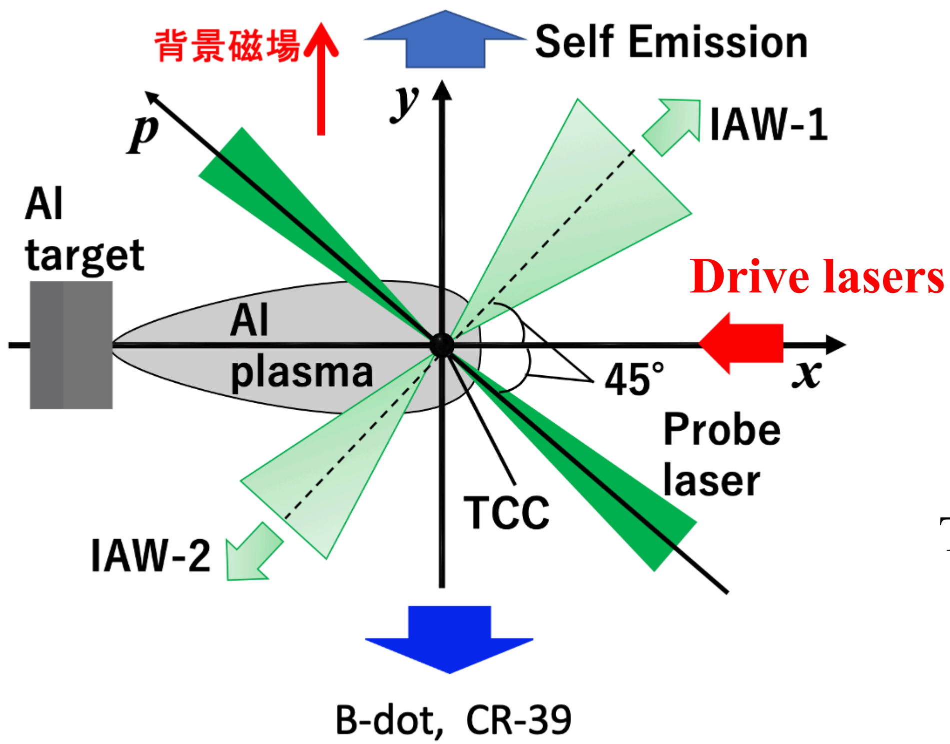

Top view (from z-axis)

Self emission imaging (B_{ext} = 0)

Self emission imaging
(shot: t=0)
FoV: ～1.5 cm 、

t = 15 ns

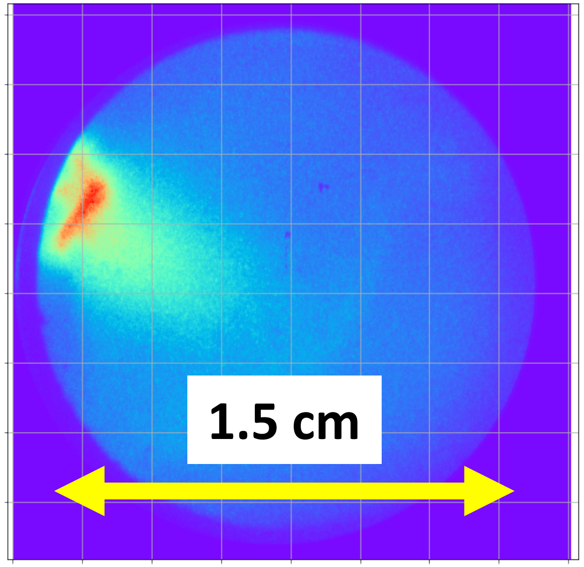

t = 20 ns

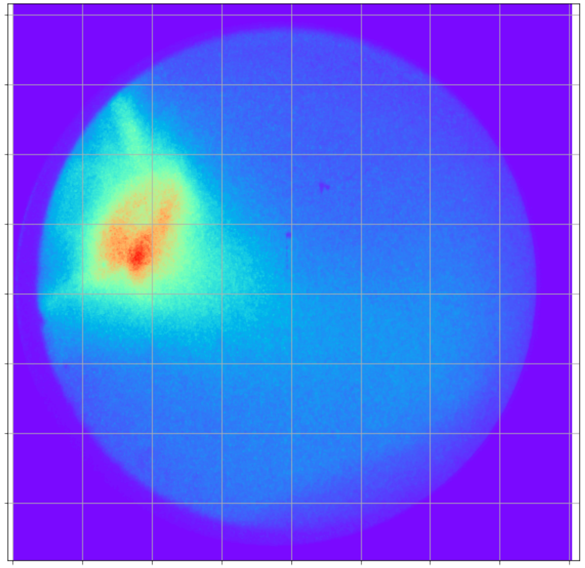

t = 26 ns

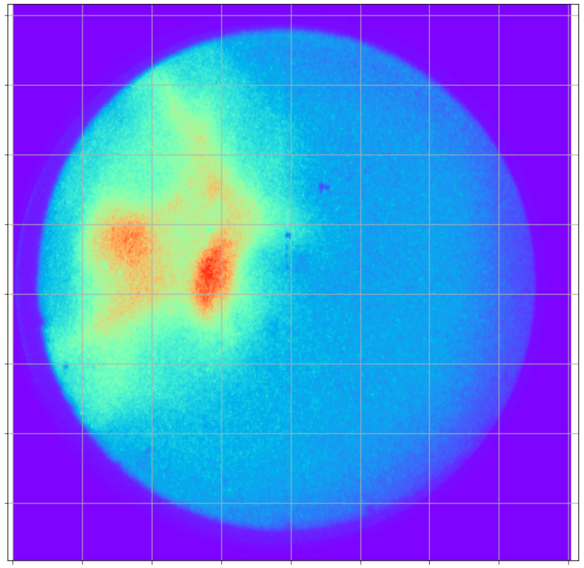

t = 32 ns

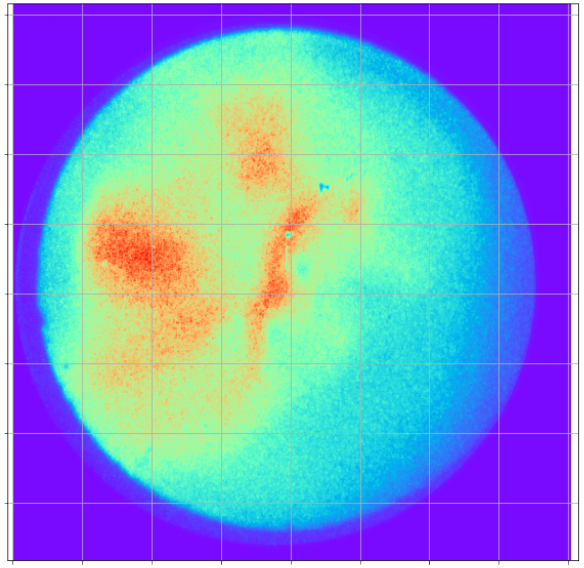

t = 37 ns

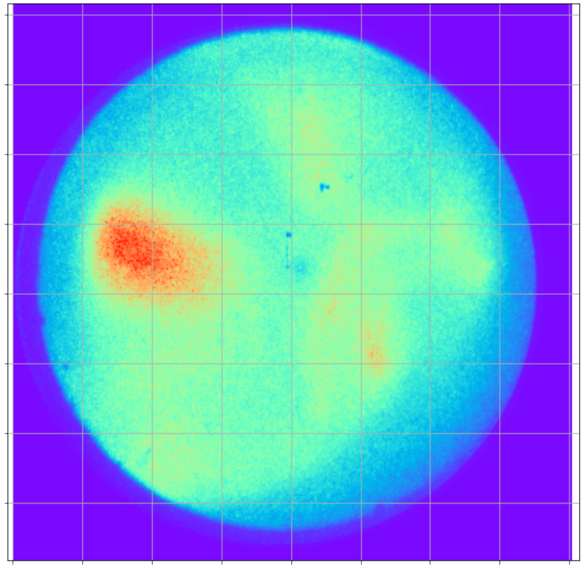

Gregori et al. 12, Nature; Kugland et al. 12, Nature Phys.:

Ablation plasma (piston plasma) is magnetized via Biermann effect.

$$\nabla T_{\mathrm{e}} \propto -\hat{r} \ , \ \nabla n_{\mathrm{e}} \propto -\hat{z}$$

$$\Rightarrow \frac{\partial \vec{B}}{\partial t} \propto (\nabla T_{\mathrm{e}} \times \nabla n_{\mathrm{e}}) \underline{\propto -\hat{\phi}}$$

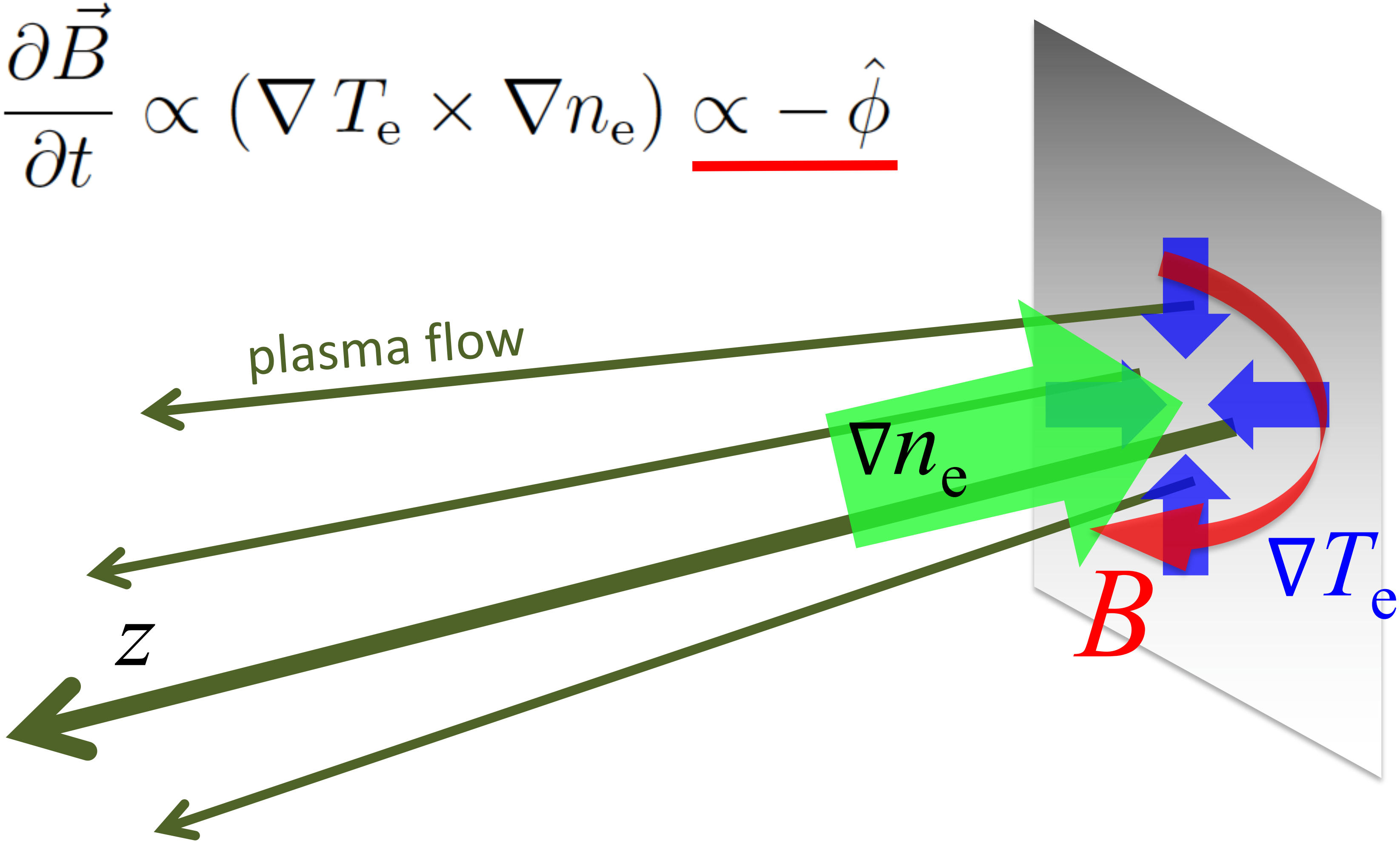

Gregori et al. 12, Nature; Kugland et al. 12, Nature Phys.:

Ablation plasma (piston plasma) is magnetized via Biermann effect.

$$\nabla T_{\mathrm{e}} \propto -\hat{r} \quad , \quad \nabla n_{\mathrm{e}} \propto -\hat{z}$$

$$\Rightarrow \quad \frac{\partial \vec{B}}{\partial t} \propto (\nabla T_{\mathrm{e}} \times \nabla n_{\mathrm{e}}) \propto -\hat{\phi}$$

$$\Rightarrow \quad B \approx \frac{T_e}{e V_d \phi}$$

$$\sim 10 \ \mathrm{T} \left(\frac{T_e}{10^3 \ \mathrm{eV}} \right) \left(\frac{V_d}{10^2 \ \mathrm{km/s}} \right)^{-1} \left(\frac{\phi_{\mathrm{f}}}{1 \ \mathrm{mm}} \right)^{-1}$$

(T_{e} : electron temp., V_{d} : flow velov., ϕ_{f} : focal spot size)

1D PIC simulations : Umeda, RY+ ('19)

Quantity	Aluminum plasma	Nitrogen plasma
Drift velocity V_d [km/s]	500	0
Magnetic field B_0 [T]		
Run 1	10.0	0.5
Run 2	10.0	0.0
Run 3	0	0.5
Run 4	0	0.0
Electrons		
Density N_e [cm^{-3}]	3.75×10^{19}	1.5×10^{18}
Plasma frequency f_{pe} [Hz]	5.51×10^{13} / 5.51×10^{12}	1.1×10^{13} / 1.1×10^{12}
Temperature T_e [eV]	10	30
Thermal velocity V_{te} [km/s]	1,330	2,300
Debye length λ_{De} [m]	3.71×10^{-9} / 3.71×10^{-8}	3.32×10^{-8} / 3.32×10^{-7}
Inertial length d_e [m]	8.39×10^{-7}	4.33×10^{-6}
Cyclotron frequency f_{ce} [Hz]	2.8×10^{11}	1.4×10^{10}
Thermal gyro radius r_e [m]	7.55×10^{-7}	2.62×10^{-5}
Plasma beta	1.62	72.99
Ions		
Charge number Z	9	3
Mass ratio m_i/m_e	49572	25704
Density N_i [cm^{-3}]	4.17×10^{18}	5.0×10^{17}
Plasma frequency f_{pi} [Hz]	7.43×10^{11} / 7.43×10^{10}	1.19×10^{11} / 1.19×10^{10}
Temperature T_e [eV]	10	30
Thermal velocity V_{ti} [km/s]	5.97	14.3
Debye length λ_{Di} [m]	3.71×10^{-9} / 3.71×10^{-8}	3.32×10^{-8} / 3.32×10^{-7}
Inertial length d_i [m]	6.23×10^{-5}	4.01×10^{-4}
Cyclotron frequency f_{ci} [Hz]	5.08×10^{7}	1.63×10^{6}
Thermal gyro radius r_i [m]	1.87×10^{-5}	1.4×10^{-3}
Alfvén velocity V_A [km/s]	19.99	4.11
Plasma beta	0.18	24.33
Grid spacing Δx [m]	8.3×10^{-8}	
Time step Δt [sec]	2.6×10^{-15}	
Number of grids N_x	120,000	
Number of steps N_t	6,000,000	
Speed of light c [km/s]	300,000 / 30,000 (laboratory) / (numerical)	

For un-magnetized Al piston plasma : B(Al) = 0 T

Ambient: B(Nitrogen) = 0

Ambient: B(Nitrogen) = 0.5 T

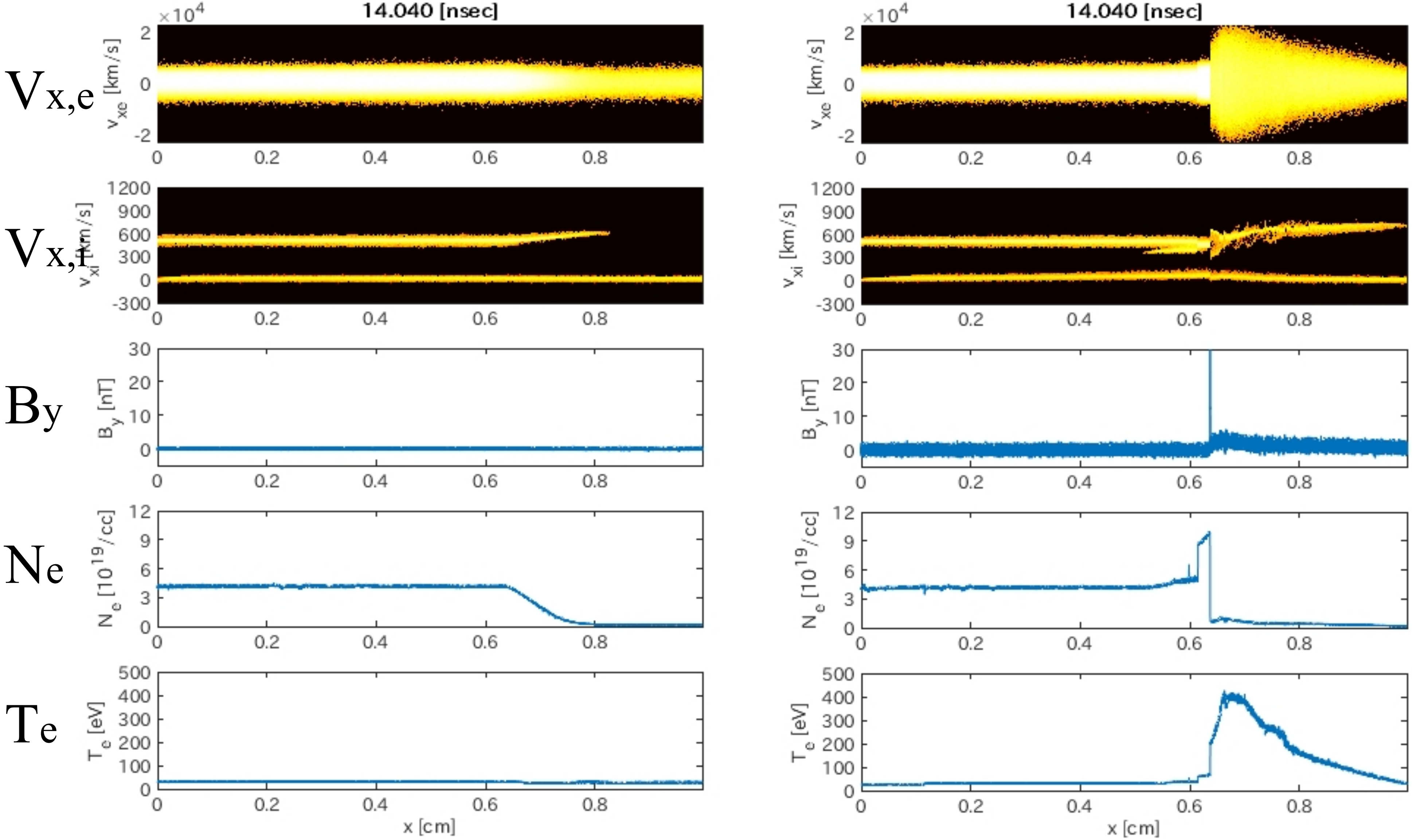

Umeda, RY, et al. 2019, PoP

瀬井柊人

Self emission imaging (B_{ext} = 0)

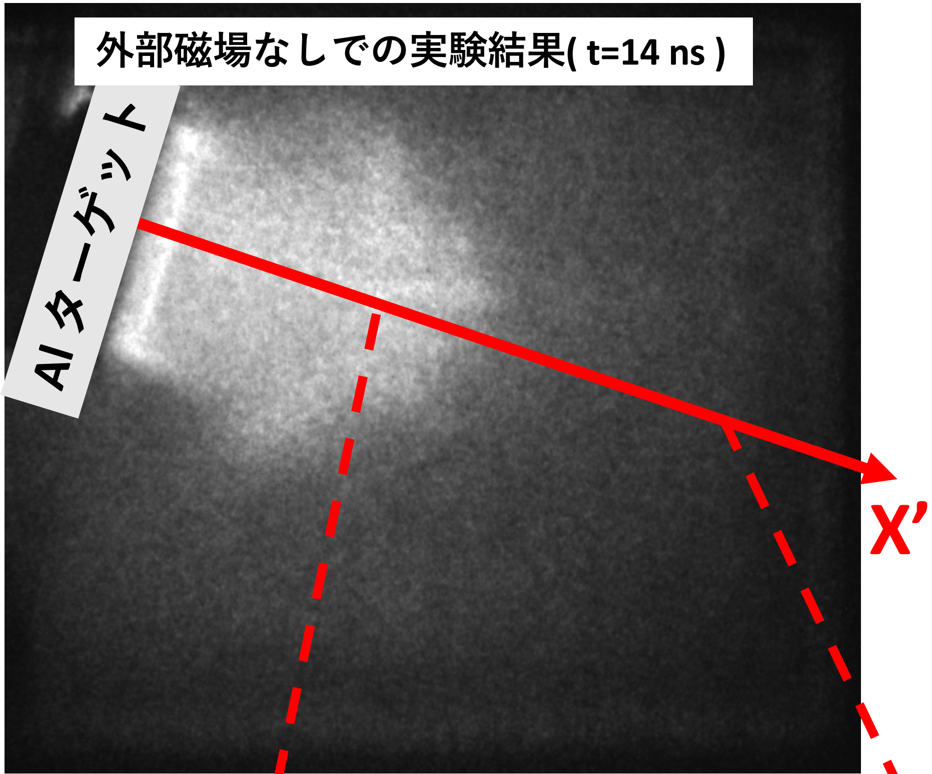

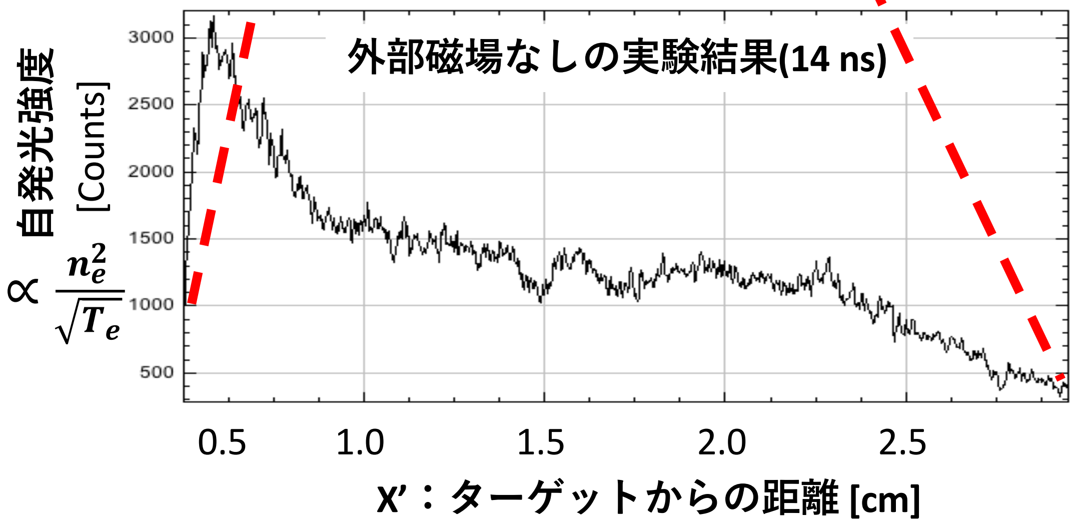

実験での自発光計測$\propto \frac{n_e^2}{\sqrt{T_e}}$において、窒素の磁場が無い場合でも、Alプラズマと窒素プラズマの相互作用が確認された。

➡Alプラズマは Biermannバッテリー効果による自己生成磁場で磁化されていると考えられる。

粒子シミュレーションの結果とも、定性的にN_e ,T_e の振る舞いが一致。

Self emission imaging (B_{ext} = 0)

Self emission imaging
(shot: t=0)
FoV: ～1.5 cm 、

t = 15 ns

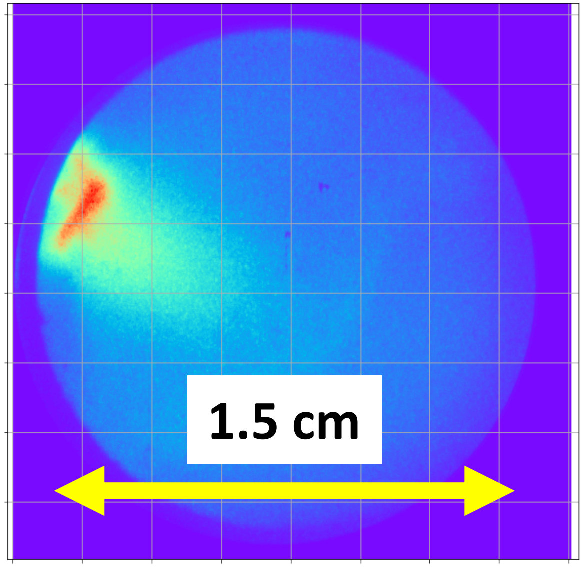

t = 20 ns

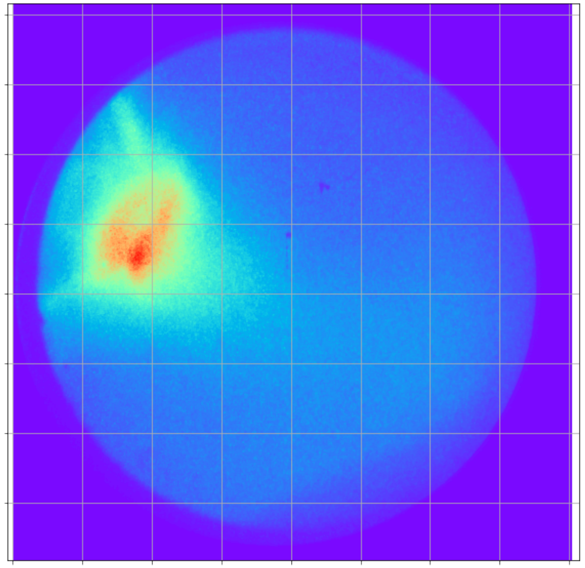

t = 26 ns

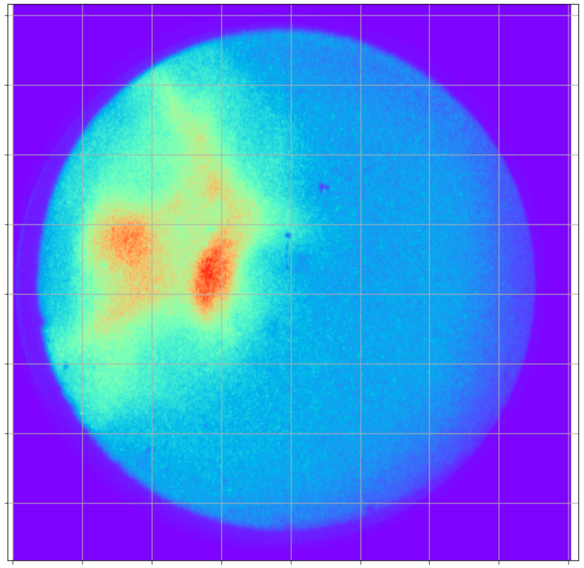

t = 32 ns

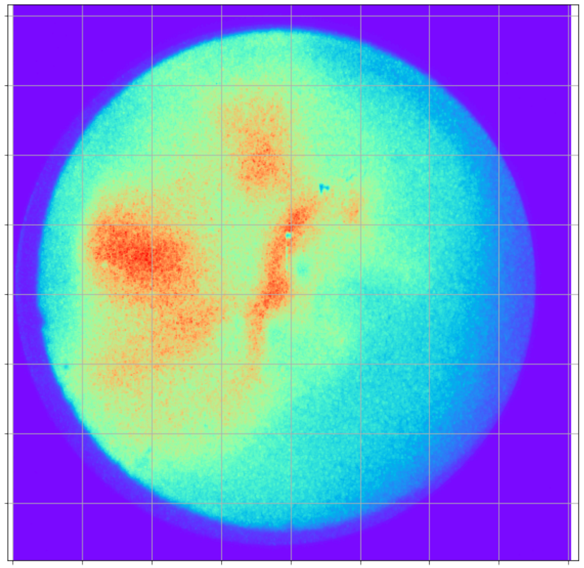

t = 37 ns

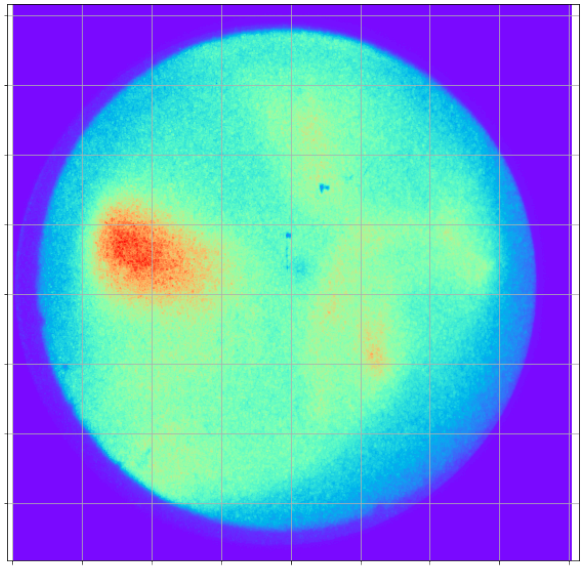

Self emission imaging (B_{ext} = 0)

Self emission imaging
(shot: t=0)
FoV: ～1.5 cm 、

: TCC.
1.4cm from target.
CTS measurement.

t = 15 ns

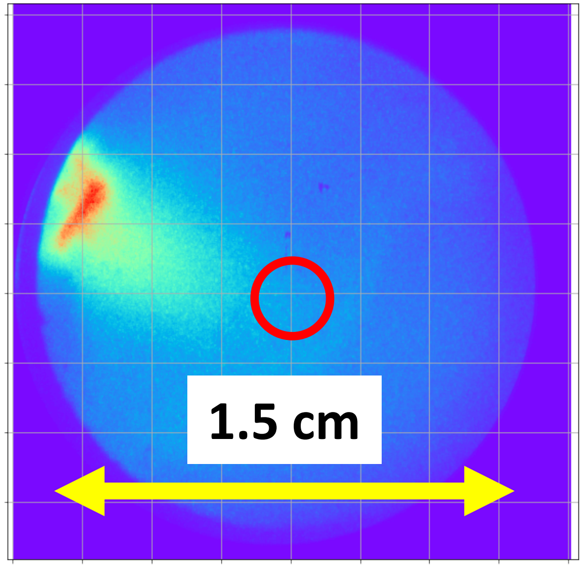

t = 20 ns

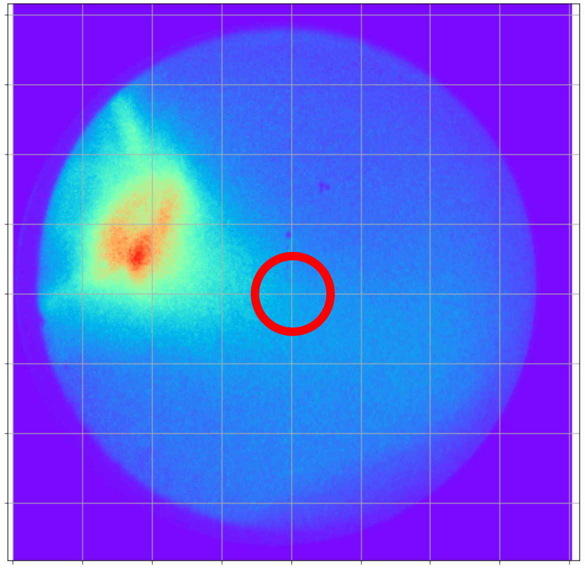

t = 26 ns

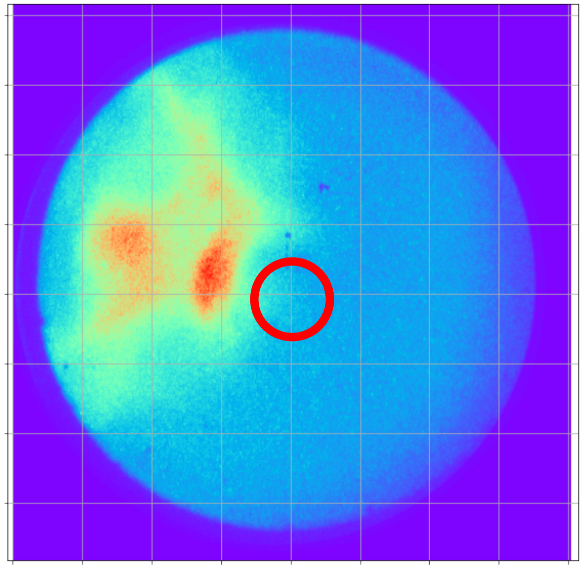

t = 32 ns

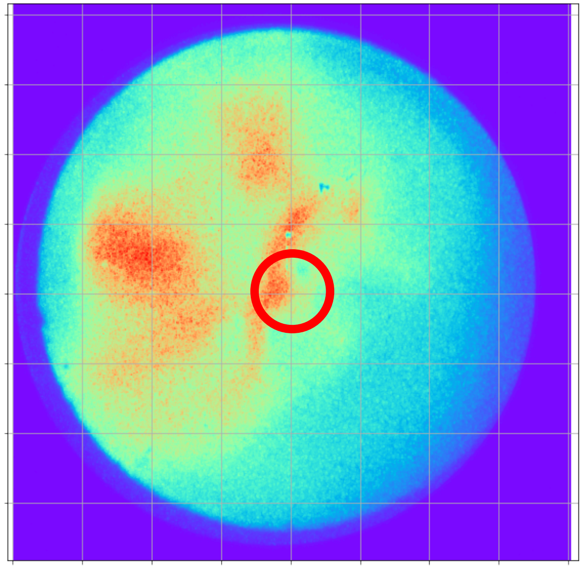

t = 37 ns

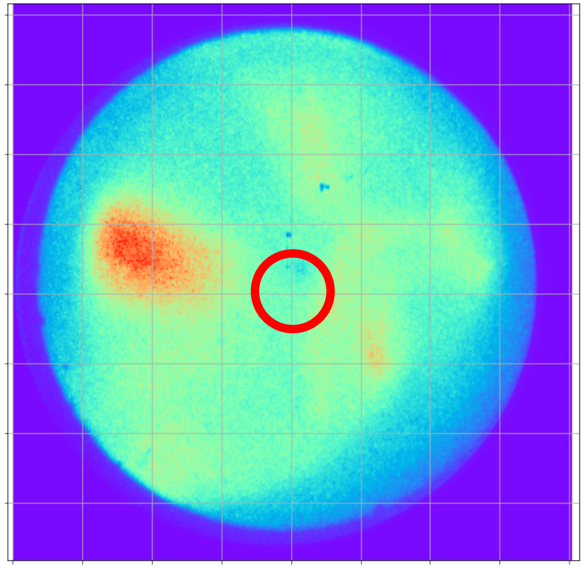

Self emission imaging (B_{ext} = 0)

Self emission imaging
(shot: t=0)
FoV: ∼1.5 cm 、

: TCC.
1.4cm from target.
CTS measurement.

t = 15 ns

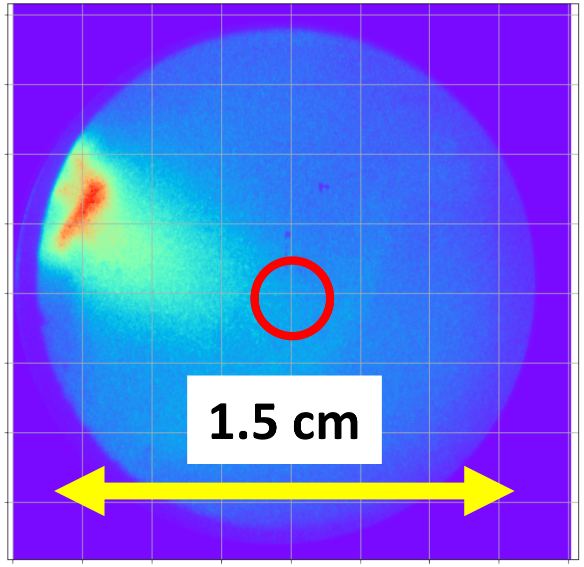

t = 26 ns

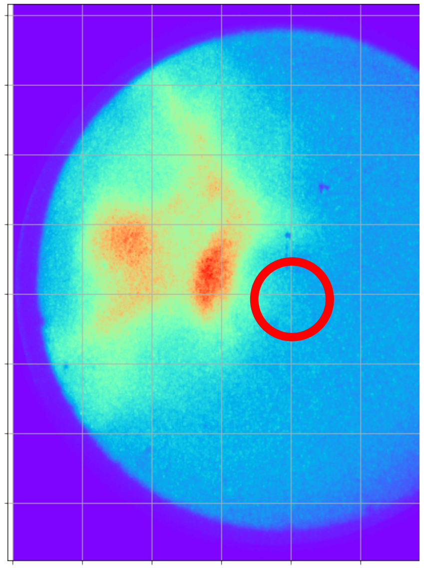

t = 32 ns

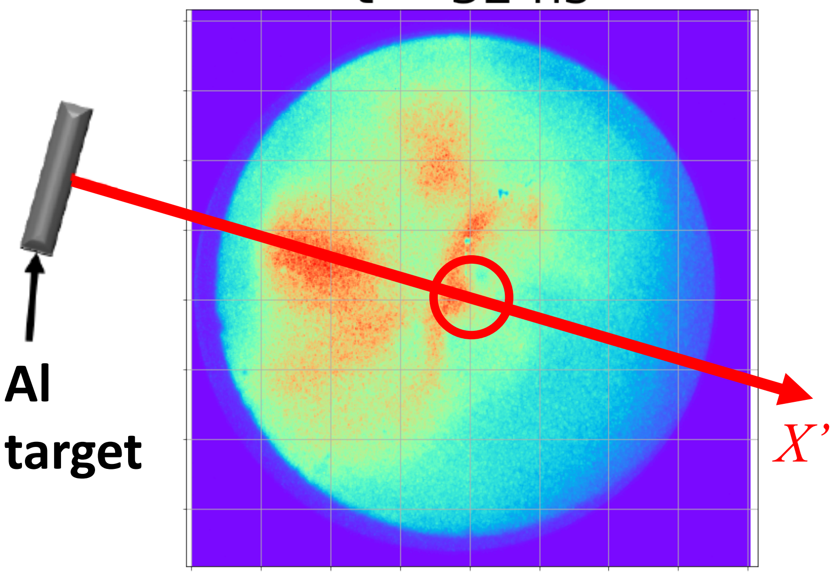

Spatio-temporal evolution along *X’* (Streaked Optical Pyrometry: SOP)

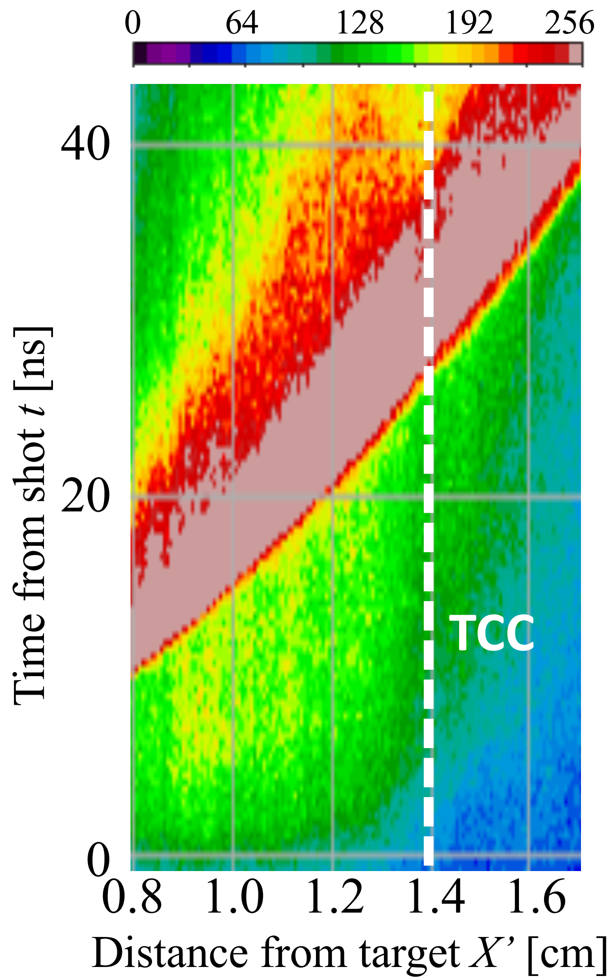

Spatio-temporal evolusion of Self emission

White circles:
time of CTS
measurements.

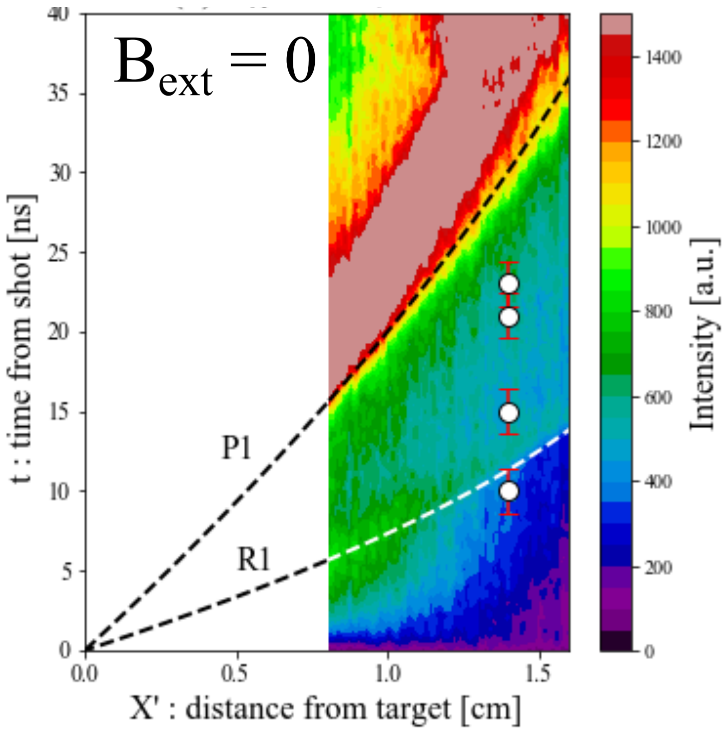

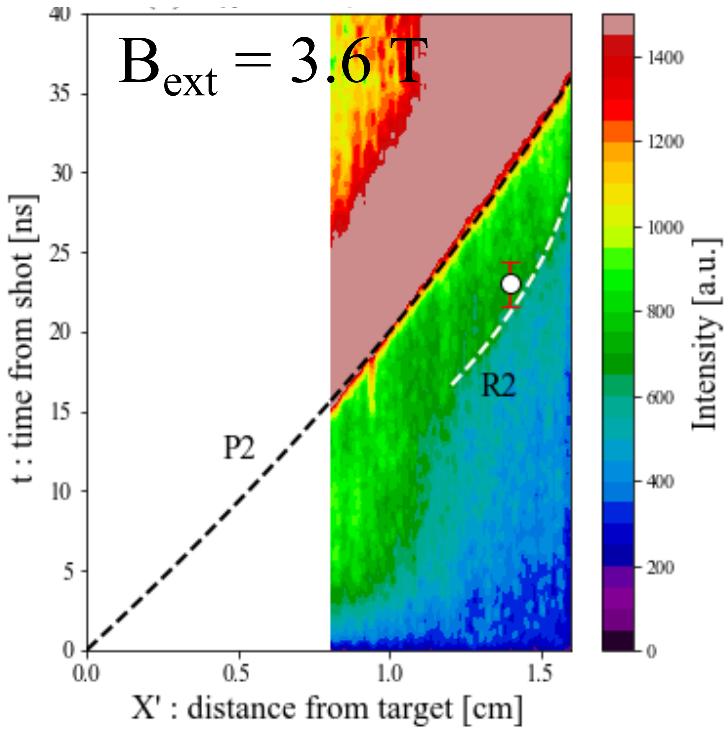

Combined w/ Thomson scattering measurement and 1D PIC simulations,

P1 & P2 (initial velocity, v_0 = 570 km/s)

=> head of Al piston (in elecfron scale).

R1 (B_{ext} = 0) (initial velocity, v_0 = 1600 km/s)

=> Al plasma penetrating into N plasmas (showing collisionless ion interaction).

R2 ($B_{ex\ t}$= 3.6 T)

=> edge of "foot" of a magnetized collisionless shock in N plasma.

Spatially resolved Thomson scattering (TS)

Collective Thomson scattering ("ion" term):

* each electrons with velocity $\vec{v}$ produces
the scattered light with frequency shift :

$$\Delta\omega = \vec{v} \cdot \vec{k}_{\mathrm{IAW}} \;,\;\; \text{where} \;\; \vec{k}_{\mathrm{IAW}} = \vec{k}_s - \vec{k}_i \;\; .$$

* "collective" means
the resonance between IAW (=ion acoustic wave)
and incident laser light (along *p*-axis).

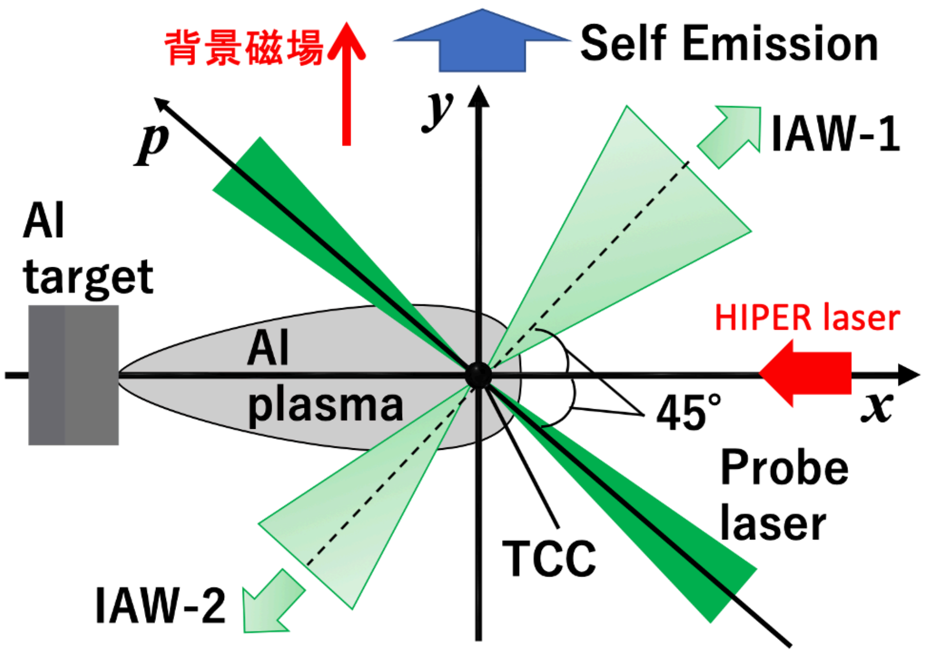

Top view (from z-axis)

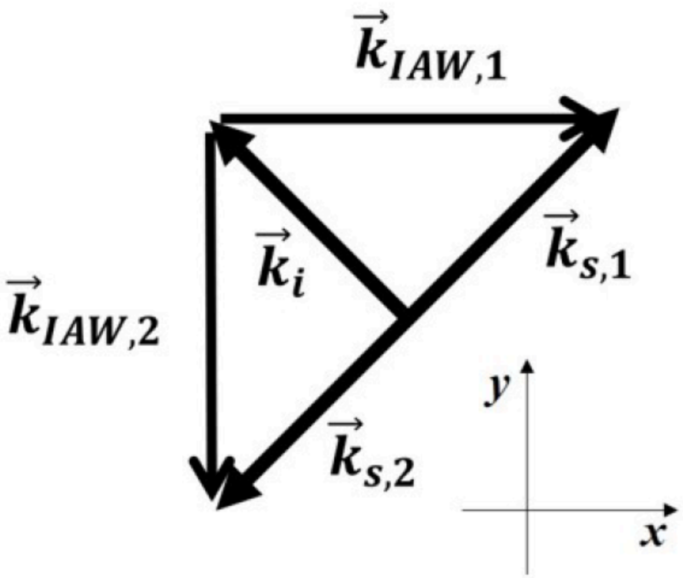

Top view (from z-axis)

Spatially resolved Thomson scattering (TS)

Collective Thomson scattering ("ion" term):

* each electrons with velocity $\vec{v}$ produces
the scattered light with frequency shift :

$$\Delta\omega = \vec{v}\cdot\vec{k}_{\rm IAW}\ ,\ \text{where}\ \ \vec{k}_{\rm IAW} = \vec{k}_s - \vec{k}_i\ .$$

* "collective" means
the resonance between IAW (=ion acoustic wave) and incident laser light (along *p*-axis).

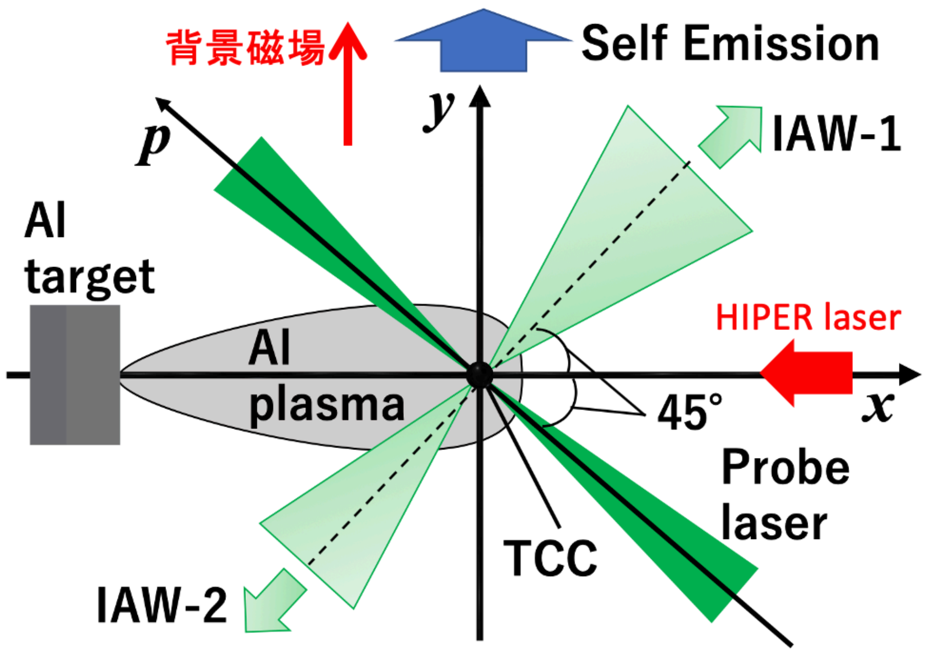

Top view (from z-axis)

Obtained data
(Incident YAG laser: 532nm)

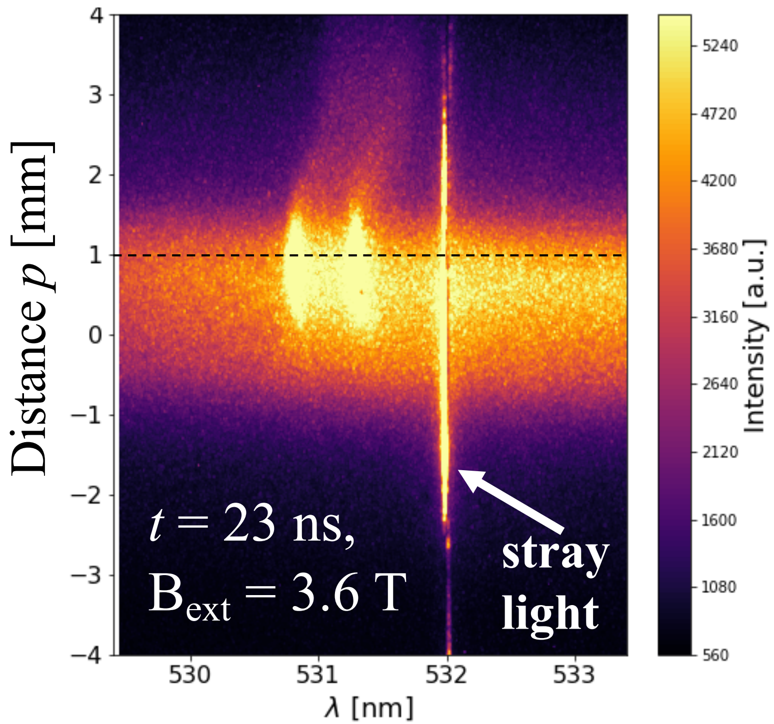

Spatially resolved Thomson scattering (TS)

Collective Thomson scattering ("ion" term):

* each electrons with velocity $\vec{v}$ produces the scattered light with frequency shift :

$$\Delta\omega = \vec{v} \cdot \vec{k}_{\mathrm{IAW}} \ , \ \text{where} \ \ \vec{k}_{\mathrm{IAW}} = \vec{k}_s - \vec{k}_i \ .$$

* "collective" means the resonance between IAW (=ion acoustic wave) and incident laser light (along *p*-axis).

TS spectrum at *p* = 1 mm

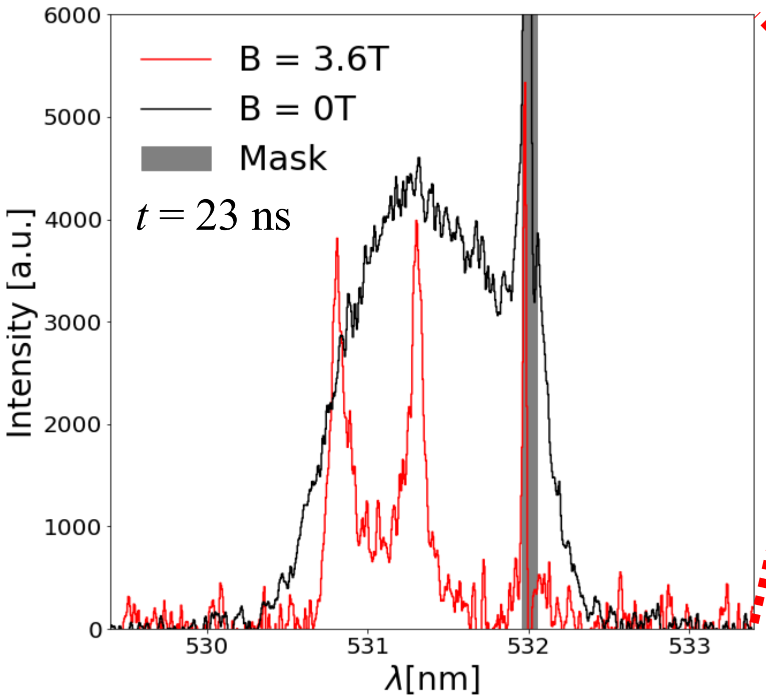

Obtained data
(Incident YAG laser: 532nm)

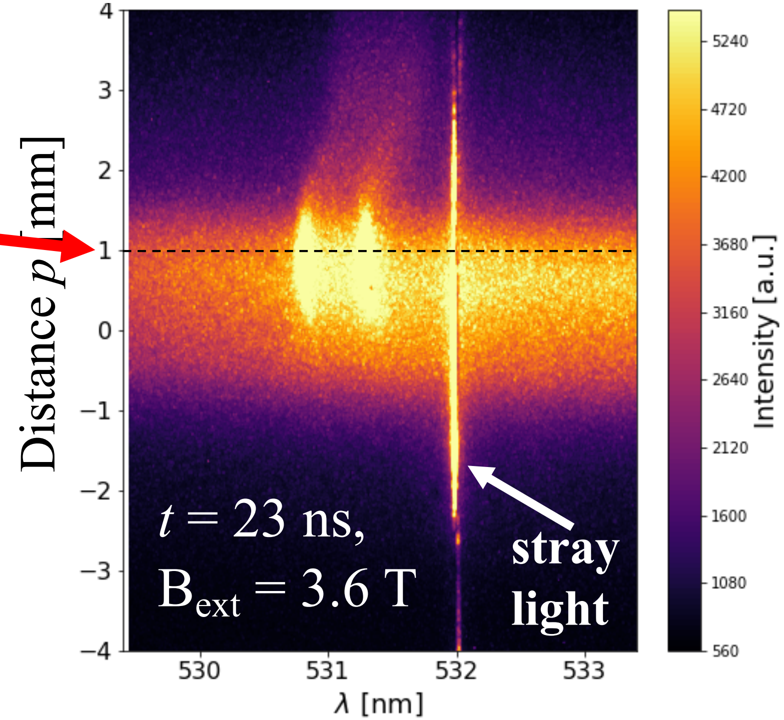

CTS spectrum fitting : B_{ext}=3.6T

Collective Thomson scattering (CTS) spectrum at p = 1 mm, 23 ns after shot (B_{ext}= 3.6 T).

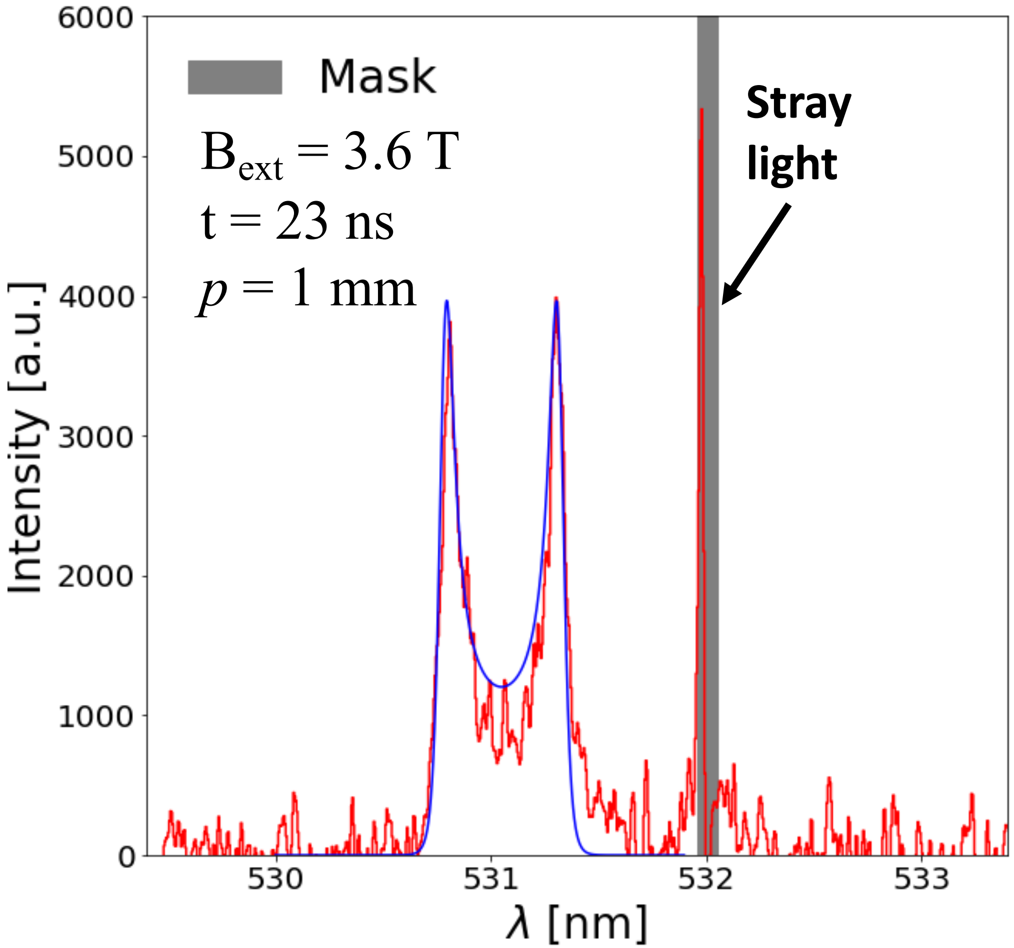

Fit w/ IAW resonance and FLYCHK:
(collision-radiative equil.)

T_e = 0.16 keV

T_i = 0.21 keV

$N_e = 7.4 \times 10^{18}$ cm^{-3}

Z = 6.4

(=> $N_{i,N} = N_e/Z = 1.2 \times 10^{18}$cm^{-3})

v = 400 km/s.

⇒ High temperature and N ion compression ($\times$3.6 ambient density).

TS spectra at TCC (p=0) for B_{ext}=0

t = 10 ns:
(blue dashed line)
Static N plasma.
Double peak with small Separation.
Fit w/ IAW/FLYCHK:
Te = Ti = 9.3eV,
Ne = 7 x 10^{17}cm^{-3},
Z = 4.2.

Warmer component can Also be seen.

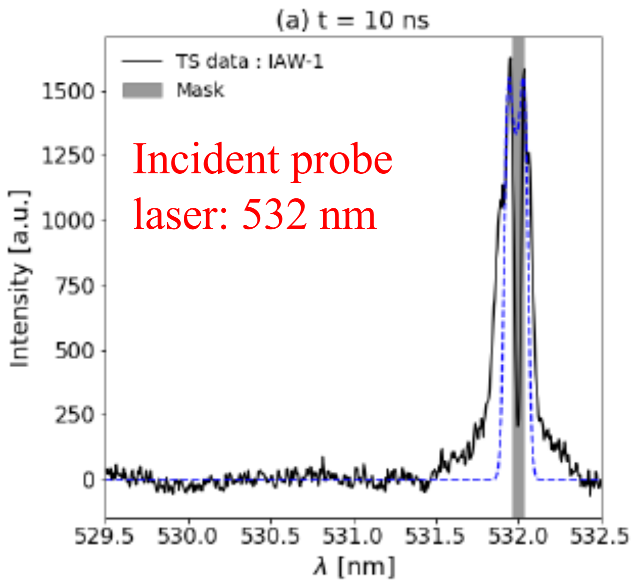

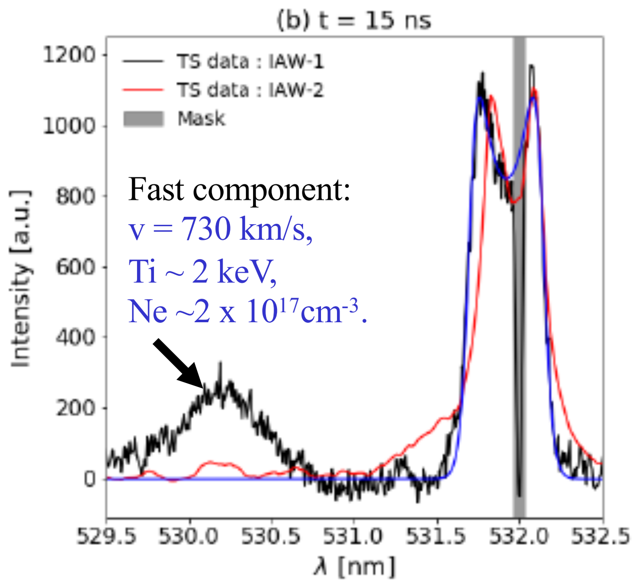

t = 15 ns:
(blue/red around 532nm)
Static N plasma.
Still double peaks.
Fit w/ IAW/FLYCHK:
Te = 98eV,
Ti = 228 eV,
Ne = 2 x 10^{18}cm^{-3},
Z = 5.5.

=> Plasma heating by "R1" seen in SOP.

t = 23 ns:
Fit with IAW resonance is impossible due to the passage of non-equilibrium plasma.

Anyway, Ti ~1 keV, with bulk velocity
v ~ 400 km/s.

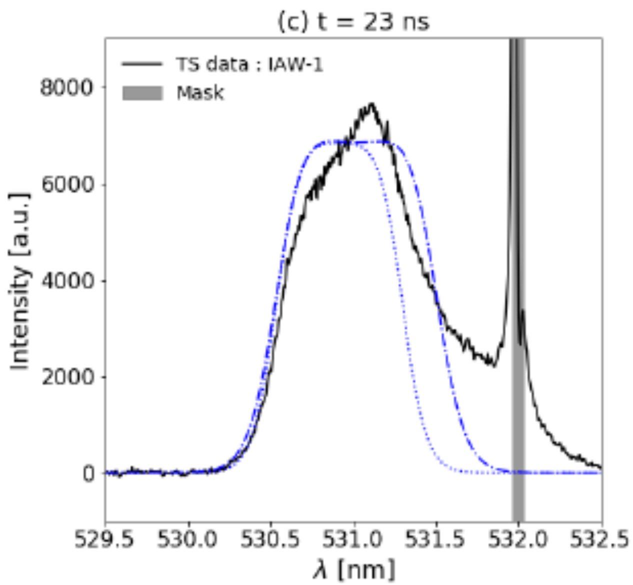

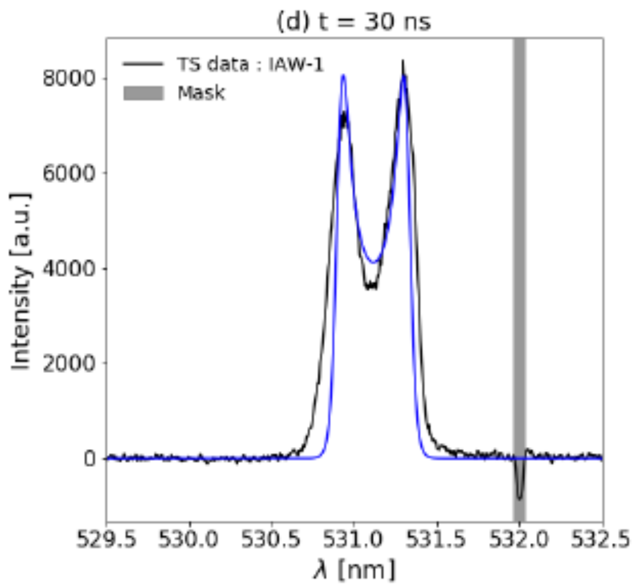

t = 30 ns:
Double peak again.
(Blue line)
Moving N plasma.
Fit with IAW/FLYCHK:
Te = 95 eV,
Ti = 166 eV,
Ne = 5 x 10^{18}cm^{-3},
Z = 5.1,
v = 360 km/s.

Identify the edge of foot: B_{ext}=3.6T

トムソン散乱計測（中央a,b）により、反射された窒素イオンのfoot先端（R2）を捉えた。
これは自発光ストリーク（左）や1次元粒子シミュレーションの結果(右c-h)とも無矛盾。

SOP (self emission)

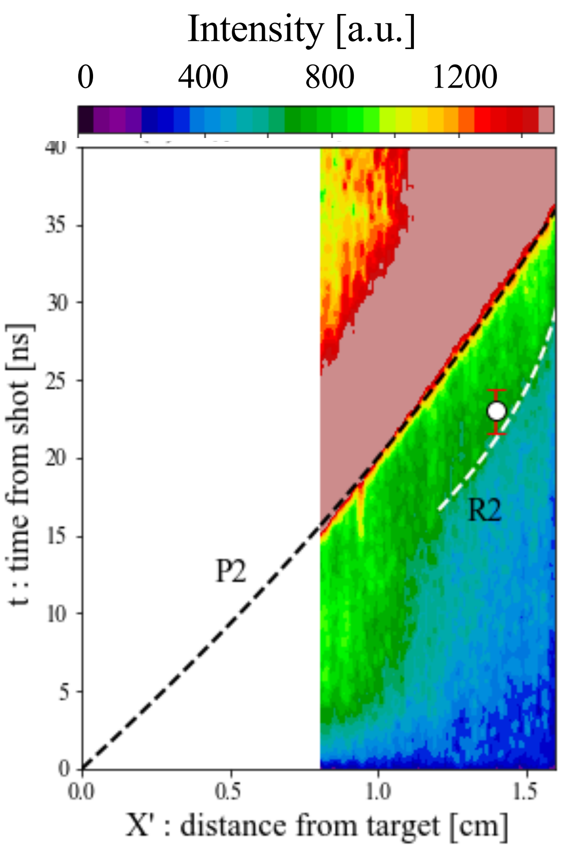

(a,b) Collective TS

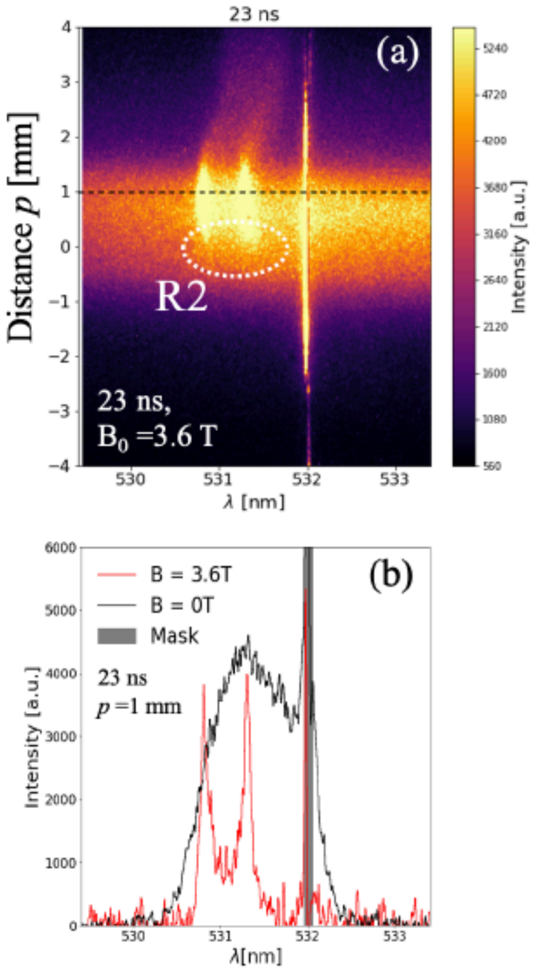

(c-h) 1D PIC simulation

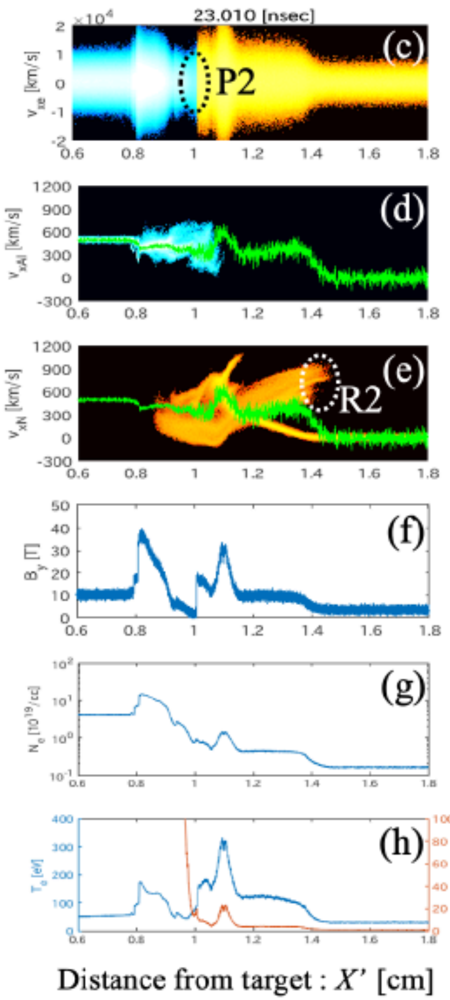

(c) Electron phase-space plot (blue: Al, yellow: N).

(d) Al ion phase-space plot. (green curve: electron bulk velocity)

(e) N ion phase-space plot (green curve: electron bulk velocity).

(f) Transverse B-field, By.

(g) Electron number density.

(h) (Blue) electron temperature. (Red) self-emission intensity.

Summary

- No external magnetic field case (B_{ext} = 0 T):
  Density jump, which is detected by SOP, is not the shock front but the electron MHD tangential discontinuity.

- External magnetic field case (B_{ext} = 3.6 T):
  * We detected an edge of shock "foot" in forming collisionless shocks with $M_A \sim M_{ms} \sim 15$, propagating into magnetized plasma at rest.

Experimental data with B_{ext} ~3.3T (4 shots) being analyzed.

This research was partially supported by:
* The joint research project of ILE Osaka University,
* JSPS KAKENHI (Grant Nos. 18H01232, 19H01868, 17H18270, 18H01245, 18H01246, 19K14712, 17J03893, 15H02154),
* JSPS Core-to-Core Program B: Asia-Africa Science Plat-forms (Grant No. JPJSCCB20190003).